

# Robust Centralized Controller Design for a Rotor System Supported by Magnetic Bearings

J. KIM AND D.-C. HAN

## ABSTRACT

This paper presents a robust centralized control scheme for a magnetic bearing system which supports a rigid rotor at both shaft ends in the radial direction. The negative stiffness element and the inductive force associated with bearing magnetic field are considered in the dynamic model of the system. For this model, the controllability and observability are examined, and then a robust control theory is applied to design two types of multi-input multi-output servocontrollers. A general servocompensator is imbedded in the first one and a centralized PID controller is suggested as a second one. By simulation study, the performance of two types of servocontrollers are compared in the aspects of the disturbance rejection, reference tracking and the robustness limit.

## 1. INTRODUCTION

The advantages of magnetic bearing application to support a rotor system are its contactless nature and active controllability. However, the active magnetic bearings are inherently unstable due to the negative stiffness elements caused by the electromagnetic field. Also, the degree of instability of the system increases according to the gyroscopic effect and the inductive forces generated in the magnetic bearings as the spinning rate of the rotor gets higher.

Another problem to deal with is the nonlinear characteristics of the electromagnetic fields. This nonlinearity results in complicated dynamic model and inevitable modeling error. Also there exist unpredictable disturbances due to mass unbalances of the rotor.

Hence, an asymptotically stable and robust cross feedback control scheme is required for magnetic bearing supported rotor systems. Recently several centralized MIMO controller designs have been developed by using the state-space model approaches [1,2]. These control schemes can easily accommodate the cross feedback capability through the utilization of the full-

Jongwon Kim and Dong-Chul Han, Institute of Advanced Machinery and Design,  
Seoul National Univ., San 56-1, Sinlim-Dong, Kwanak-Ku, Seoul 151-742, KOREA

state feedback elements with observers. However, one of main claims against these approaches is that the robustness is not guaranteed in the entire operating range over which the modeling error and unpredictable disturbances may occur [3].

In this paper, the robust control theory suggested by Davison [4] is applied to design a centralized controller for a rigid rotor supported by magnetic bearings. A general servocompensator is imbedded into the MIMO control scheme for the perfect rejection and tracking of the sinusoidal type disturbances and reference signals, respectively. Also, a centralized PID controller is suggested as a simpler version of the previous one.

The dynamic model of the rigid rotor system in magnetic bearings is summarized in Section 2. Section 3 briefly shows the implementation of the control schemes, and the simulation results are presented in Section 4, where the performance comparison between two types of controllers and the robustness limit against the change of rotor dynamics are described.

## 2. MODELLING OF A ROTOR SYSTEM IN MAGNETIC BEARINGS

The schematic model of a rigid rotor system supported by magnetic bearings is shown in Fig.1. The inertia is at a distance  $L_1$  and  $L_2$  from left and right side support respectively. The spin axis of the rotor is taken to be x-axis with clockwise spin being a positive angular rotation speed  $\omega_x$ .

The inertia of the rotor about the x-axis is  $J_a$  and that about y and z-axis is  $J_r$ . It is assumed in the analysis that the pitch and yaw angles are sufficiently small and that the values of  $J_a$  and  $J_r$  are independent of rotor motion. The mass of the rotor is  $M$  and it is assumed that the shaft is massless.

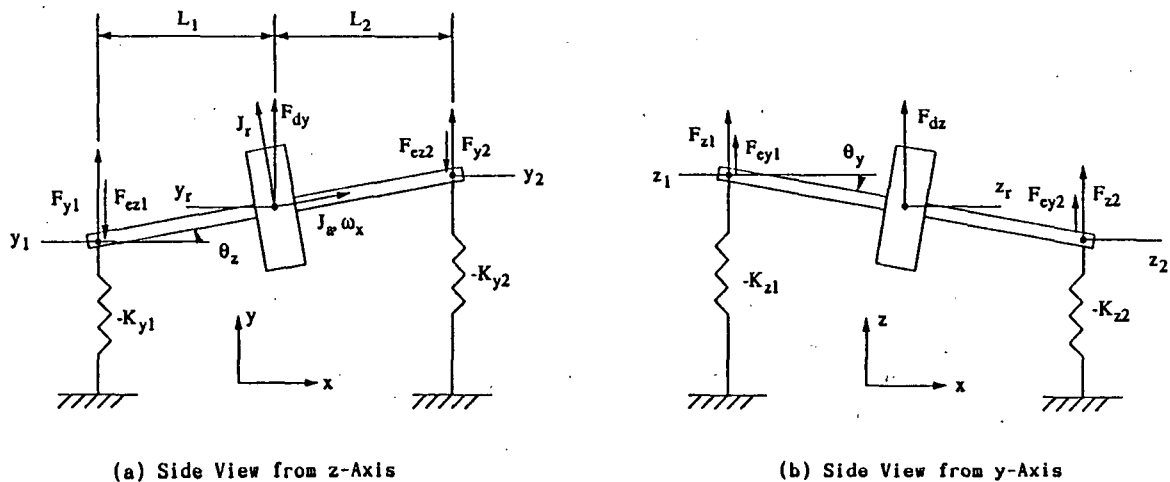


Fig.1 A Rigid Rotor Model Supported by Magnetic Bearings

From Fig.1, the equations for the translational motion of the rotor are

$$(F_{y1} + K_{y1} y_1 - F_{ez1}) + (F_{y2} + K_{y2} y_2 - F_{ez2}) + F_{dy} = M \ddot{y}_r \quad (1)$$

$$(F_{z1} + K_{z1} z_1 + F_{ey1}) + (F_{z2} + K_{z2} z_2 + F_{ey2}) + F_{dz} = M \ddot{z}_r \quad (2)$$

where the  $F_i$  and  $F_{ei}$  ( $i=y_1, y_2, z_1, z_2$ ) are the magnetic force inputs and the inductive forces, respectively.  $F_{ei}$  is described as

$$F_{ei} = K_{ei} \omega_x i \quad (3)$$

where  $K_{ei}$  are the inductive force coefficients and  $\omega_x$  is the spinning speed of the rotor shaft.  $F_{dy}$ ,  $F_{dz}$  are the disturbances to the rotor mass and  $K_i$  are the magnetic bearing stiffnesses at each set of poles.

Also the equations for the rotational motion are

$$L_2(F_{y2} + K_{y2} y_2 - F_{ez2}) - L_1(F_{y1} + K_{y1} y_1 - F_{ez1}) = J_r \ddot{\theta}_z - J_a \omega_x \dot{\theta}_y \quad (4)$$

$$-L_2(F_{z2} + K_{z2} z_2 + F_{ey2}) + L_1(F_{z1} + K_{z1} z_1 + F_{ey1}) = J_r \ddot{\theta}_y + J_a \omega_x \dot{\theta}_z \quad (5)$$

where  $\theta_y$  is the yaw angle about y-axis and  $\theta_z$  is the pitch angle about z-axis and from geometry

$$y_1 = y_r - L_1 \theta_z ; \quad y_2 = y_r + L_2 \theta_z \quad (6)$$

$$z_1 = z_r + L_1 \theta_y ; \quad z_2 = z_r - L_2 \theta_y \quad (7)$$

Now following assumptions are made without loss of generality:

$$K_{ez1} = K_{ey1} \equiv K_{e1} ; \quad K_{ez2} = K_{ey2} \equiv K_{e2} \quad (8)$$

$$K_{y1} = K_{z1} \equiv K_{m1} ; \quad K_{y2} = K_{z2} \equiv K_{m2} \quad (9)$$

then, with following definitions

$$p = J_a/J_r ; \quad \omega_{t1}^2 = K_{m1}/M ; \quad \omega_{t2}^2 = K_{m2}/M ; \quad \omega_{a1} = K_{e1}/M ; \quad \omega_{a2} = K_{e2}/M \quad (10)$$

$$L = L_1 + L_2 ; \quad \alpha = L_1/L \quad (11)$$

$$\omega_{r1}^2 = L^2 K_{m1}/J_r ; \quad \omega_{r2}^2 = L^2 K_{m2}/J_r ; \quad \omega_{b1} = L^2 K_{e1}/J_r ; \quad \omega_{b2} = L^2 K_{e2}/J_r \quad (12)$$

the system equations of the rigid rotor supported by magnetic bearings can be summarized into a state-space model :

$$\dot{x} = A x + B u + E \omega \quad (13)$$

$$y = C x \quad (14)$$

where the matrices A, B, E and C are shown in Fig.2. Here, x is the state variable vector defined as

$$\{ x \}^T = \{ y_r, y_d, z_r, z_d, \dot{y}_r, \dot{y}_d, \dot{z}_r, \dot{z}_d \} \quad (15)$$

where  $y_d = L \theta_z$  and  $z_d = L \theta_y$ . y is the regulated output defined as

$$(16)$$

0				I			
$\omega_{t1}^2 + \omega_{t2}^2$	$-\alpha\omega_{t1}^2 + (1-\alpha)\omega_{t2}^2$	$-(\omega_{a1} + \omega_{a2}) * \omega_x$	$\{-\alpha\omega_{a1} + (1-\alpha)\omega_{a2}\} * \omega_x$	0	0	0	0
$-\alpha\omega_{r1}^2 + (1-\alpha)\omega_{r2}^2$	$\alpha^2\omega_{r1}^2 + (1-\alpha)^2\omega_{r2}^2$	$\{\alpha\omega_{b1} - (1-\alpha)\omega_{b2}\} * \omega_x$	$\{\alpha\omega_{b1} + (1-\alpha)\omega_{b2}\} * \omega_x$	0	0	0	$p\omega_x$
$(\omega_{a1} + \omega_{a2}) * \omega_x$	$\{-\alpha\omega_{a1} + (1-\alpha)\omega_{a2}\} * \omega_x$	$\omega_{t1}^2 + \omega_{t2}^2$	$\alpha\omega_{t1}^2 - (1-\alpha)\omega_{t2}^2$	0	0	0	0
$\{\alpha\omega_{b1} - (1-\alpha)\omega_{b2}\} * \omega_x$	$\{-\alpha\omega_{b1} - (1-\alpha)\omega_{b2}\} * \omega_x$	$\alpha\omega_{r1}^2 - (1-\alpha)\omega_{r2}^2$	$\alpha^2\omega_{r1}^2 + (1-\alpha)^2\omega_{r2}^2$	0	$-p\omega_x$	0	0

(a) Matrix A

0			
$\frac{1}{M}$	0	$\frac{1}{M}$	0
$\frac{L a}{J_r}$	0	$\frac{L(1-a)}{J_r}$	0
0	$\frac{1}{M}$	0	$\frac{1}{M}$
0	$\frac{L a}{J_r}$	0	$\frac{-L(1-a)}{J_r}$

(b) Matrix B

0	
$\frac{1}{M}$	0
0	0
0	$\frac{1}{M}$
0	0

(c) Matrix E

1	-a	0	0	0	0	0	0
0	0	1	a	0	0	0	0
1	1-a	0	0	0	0	0	0
0	0	1	a-1	0	0	0	0

(d) Matrix C

Fig.2 System Matrices for a Rigid Rotor System in Magnetic Bearings

$$\{ y \}^T = \{ y_1, y_2, z_1, z_2 \} \quad (16)$$

and  $u$  is the plant inputs such as

$$\{ u \}^T = \{ F_{y1}, F_{z1}, F_{y2}, F_{z2} \} \quad (17)$$

$\omega$  is the disturbances to the rotor mass defined as

$$\{ \omega \}^T = \{ F_{dy}, F_{dz} \} \quad (18)$$

The controllability matrix can be given by

$$C_o = [ B, AB ] \quad (19)$$

and  $\det[C_o] = \alpha^4 / J_r^4 M^4 \quad (20)$

Thus,  $\det[C_o]$  is positive, and the plant is controllable for any choice of plant parameters except for the case  $\alpha = 0$ , which means that the plant requires two separate bearings to be controllable.

The observability matrix can be given by

$$O_b = \begin{bmatrix} C \\ CA \end{bmatrix} \quad (21)$$

and  $\det[O_b] = 1 \quad (22)$

Thus, the plant is always observable.

### 3. STRUCTURE OF ROBUST CENTRALIZED CONTROLLER

The general servocompensator [5] which is to be used in this application is specifically defined as follows with input  $e \in R^4$  and output  $\eta \in R^{12}$

$$\dot{\eta} = C^* \eta + B^* e; \quad e \equiv y_{ref} - y \quad (23)$$

where

$$C^* \equiv \text{blockdiag} (C_p, C_p, C_p, C_p) \quad (24)$$

$$B^* \equiv \text{blockdiag} (B_p, B_p, B_p, B_p) \quad (25)$$

and  $C_p$  and  $B_p$  are defined as

$$C_p \equiv \begin{bmatrix} 0 & 1 & 0 \\ 0 & 0 & 1 \\ 0 & -\omega_x^2 & 0 \end{bmatrix} \quad \text{and} \quad B_p \equiv \begin{bmatrix} 0 \\ 0 \\ 1 \end{bmatrix} \quad (26)$$

The servocompensator is then combined with the plant (13) and (14) to yield

the following system:

$$\begin{bmatrix} \dot{x} \\ \dot{\eta} \end{bmatrix} = \begin{bmatrix} A & 0 \\ -B^*C & C^* \end{bmatrix} \begin{bmatrix} x \\ \eta \end{bmatrix} + \begin{bmatrix} B \\ 0 \end{bmatrix} u + \begin{bmatrix} E & 0 \\ 0 & B^* \end{bmatrix} \begin{bmatrix} \omega \\ y_{ref} \end{bmatrix} \quad (27)$$

$$\begin{bmatrix} y \\ \eta \end{bmatrix} = \begin{bmatrix} C & 0 \\ 0 & I \end{bmatrix} \begin{bmatrix} x \\ \eta \end{bmatrix} \quad (28)$$

Then any robust controller for (13) and (14) must have the following structure [4,5] :

$$u = K_o \hat{x} + K \eta \quad (29)$$

where  $\hat{x}$  is the output of an observer of order  $\hat{n} \leq 8$  with input  $y$  and  $u$ .

$K_o$ ,  $K$  can be found by using pole assignment method (or linear quadratic optimal control theory) to stabilize and give desired transient behavior for the system (27) and (28) if and only if the following "plant conditions" all hold:

- (1)  $(C, A, B)$  has no unstable fixed modes [6].
- (2) The transmission zeros of  $(C, A, B, 0)$  do not coincide with  $\lambda = 0, \pm \omega_{xi}$ .
- (3) The outputs  $y$  are physically measurable.

The general servocompensator defined in (23) can be reduced to include only the integrator terms as follows :

$$\dot{\eta} = e : e \equiv y_{ref} - y \quad (30)$$

where  $\eta \in R^4$ , then a MIMO centralized PID type control scheme is obtained.

#### 4. SPECIFIC DESIGN EXAMPLES

In this section, specific examples of robust centralized controllers are given for a rigid rotor in magnetic bearings. The rotor parameters are same as those in the work of Fermental et al. [7] :

$$M = 100 \text{ [kg]}, \quad L_1 = L_2 = 1 \text{ [m]}, \quad J_r = J_a = 1 \text{ [kgm}^2\text{]} \quad (31)$$

and the magnetic bearing stiffnesses and inductive force coefficients are assumed to be

$$K_m \equiv K_{m1} = K_{m2} = 8 \times 10^6 \text{ [N/m]} \quad (32)$$

$$K_e \equiv K_{e1} = K_{e2} = 500 \text{ [Ns/m]} \quad (33)$$

Then

$$p = 1; \quad \omega_{t1} = \omega_{t2} = 283 \text{ [r/s]}; \quad \omega_{a1} = \omega_{a2} = 5 \text{ [r/s]}; \quad (34)$$

$$\omega_{r1} = \omega_{r2} = 2830 \text{ [r/s]}; \quad \omega_{b1} = \omega_{b2} = 500 \text{ [r/s]} \quad (35)$$

The "plant conditions" in Section 3 should be satisfied for a robust

controller to exist. It is known [6] that (C,A,B) has no fixed modes if and only if (C,A,B) is controllable and observable. The eight transmission zeros of the plant are located very far from the origin with each of three zeros is along the positive and negative imaginary axis, respectively, and the other two zeros are along the each direction of the real axis. So, these zeros do not coincide with  $\lambda = 0, \pm \omega_x i$ . Since the regulated outputs  $y$  are measurable, the "plant conditions" are satisfied.

The locus of the open-loop eigenvalues of system matrix A are shown in Fig.3. The open-loop system is highly unstable due to the negative stiffness of magnetic bearings. The inner boundary to the origin and the 'x' are the locus when the  $\omega_x$  increases from 0 to 6000 r/s with  $\alpha = 0.5$ . The open-loop poles are at  $s = \pm 400$ , and  $s = \pm 2000$  at  $\omega_x = 0$  r/s, which correspond to the resonance frequencies of

$$\omega_{o1} = [ 2 K_m/M ]^{1/2} \quad \text{and} \quad \omega_{o2} = [ L^2 K_m / 2 J_r ]^{1/2} \quad (36)$$

In general, the resonance frequencies at  $\omega_x = 0$  r/s and  $\alpha = \alpha_1$  are

$$\omega_o = [ \omega_s^2/2 \pm 0.5 \{ \omega_s^4 - 4 (K_m/M) (L^2 K_m/J_r) \}^{1/2} ]^{1/2} \quad (37)$$

where 
$$\omega_s^2 = 2 K_m/M + L^2 K_m/J_r [(1-\alpha_1)^2 + \alpha_1^2] \quad (38)$$

The outer boundary to the origin and the 'o' are the locus when  $\alpha = 1.0$ . The open-loop poles start from the real axis (at  $s = \pm 281$  and  $\pm 2830$ ) and breaks out into the direction to the imaginary axis as  $\omega_x$  increases.

The closed-loop poles are assigned such that the damping coefficient should be 0.707 and that resultant natural frequencies do not coincide with the open-loop resonance frequencies :

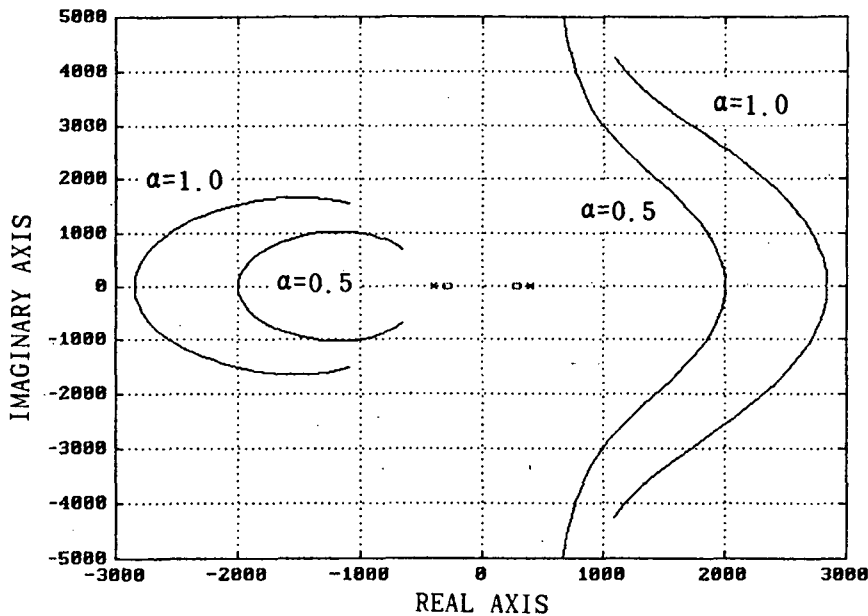


Fig.3 Locus of Open-loop Poles of System Matrix A

$$P_{1,2,3,4} = -140; \quad P_{5,6,7,8} = -100 \pm 100j; \quad P_{9,10,11,12} = -3000 \quad (39)$$

for both of the general servocompensator and the centralized PID control schemes. For the additional poles for the general servocompensator, followings are assigned :

$$P_{13,14,15,16} = -1000; \quad P_{17,18,19,20} = -1000 \pm 300j \quad (40)$$

The simulation result for testing disturbance rejection is shown in Fig.4. In this case, a sinusoidal type disturbance  $F_{dy} = 1000 \sin(\omega_x t)$  [N] is applied to the rotor mass, and the reference signals are  $y_{1ref} = 0.0002$  [m] and  $y_{2ref} = -0.0002$  [m] with  $\omega_x = 400$  [r/s]. In Fig.4 (a), it is verified that a perfect regulation can be achieved by using the general servocompensator. In case of centralized PID controller, in Fig.4 (c), a steady-state error cannot be avoided. In Fig.4 (b) and (d), the magnitudes of the control inputs of the two control schemes are almost same with each other at steady-state.

Fig.5 shows the results of the sinusoidal reference tracking to make the geometrical axis of the rotor whirl around the bearing center axis with each shaft ends at  $180^\circ$  phase shift. The disturbance  $F_{dy} = -1000$  [N] is exerted along the  $y_1$ -axis. The first one yields a perfect tracking, whereas the second one produces an elliptical motion. The rotating direction is also reversed in case of second one because of the phase lag of the  $y_1$ -axis caused by the disturbance.

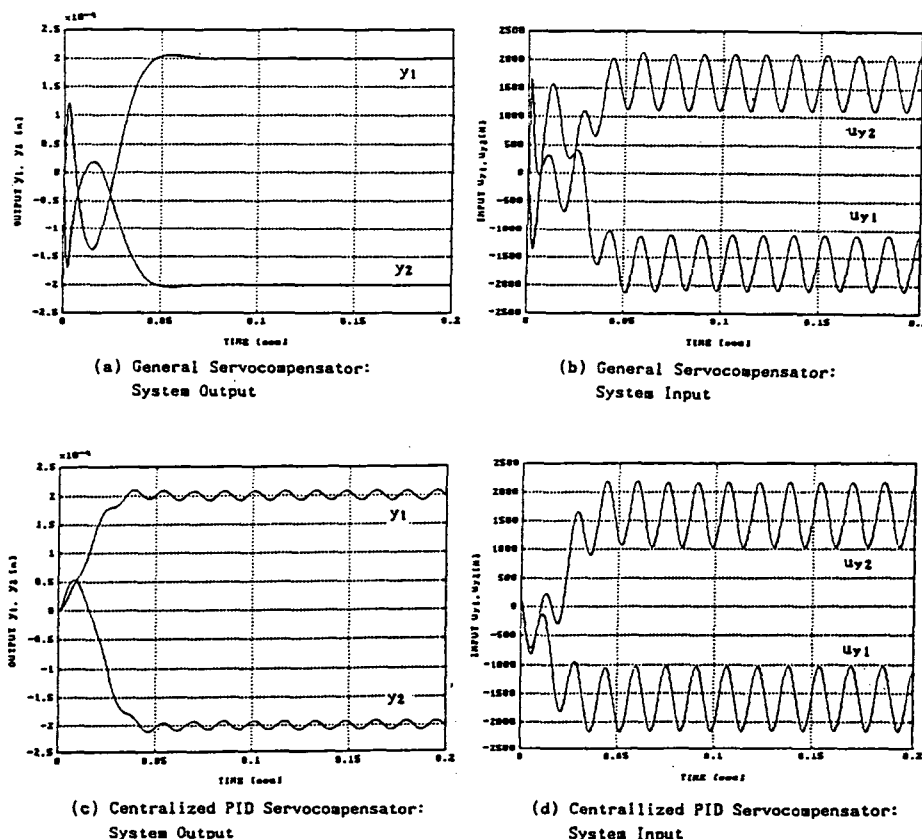
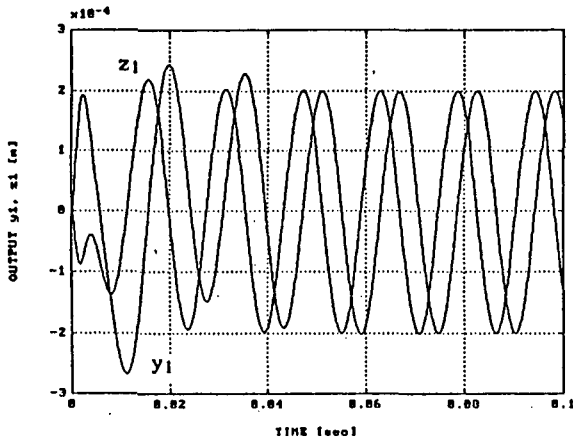
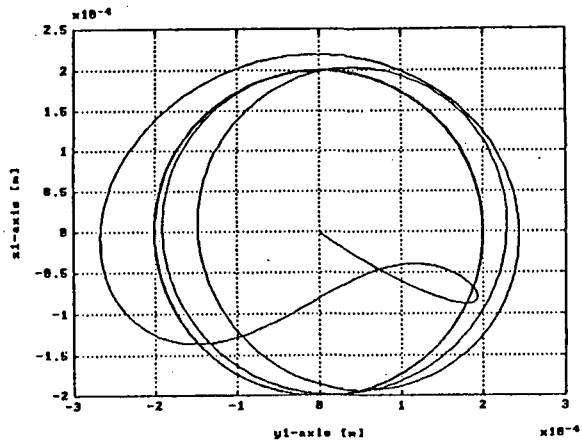


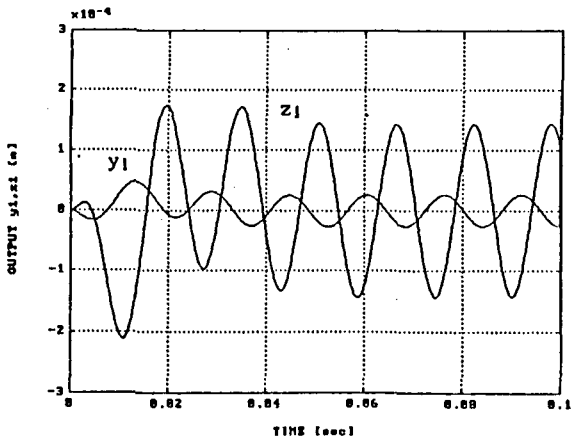
Fig.4 Simulation Results for Sinusoidal Disturbance Rejection  
(  $y_{1ref}=0.0002$ [m],  $y_{2ref}=-0.0002$ [m],  $F_{dy}=1000\sin(400t)$ [N] )



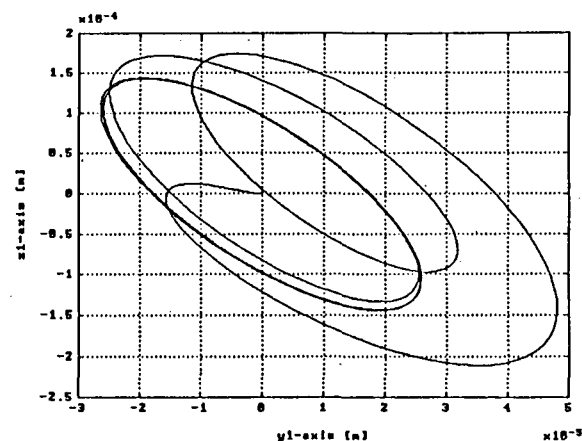
(a) General Servocompensator:  
System Output



(b) General Servocompensator:  
Axis Trajectory

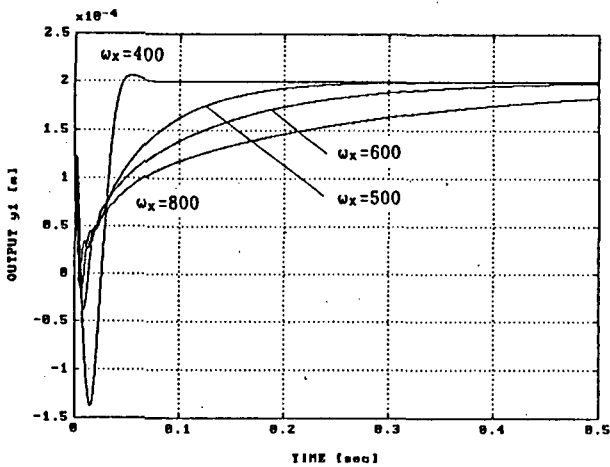


(c) Centralized PID Servocompensator:  
System Output

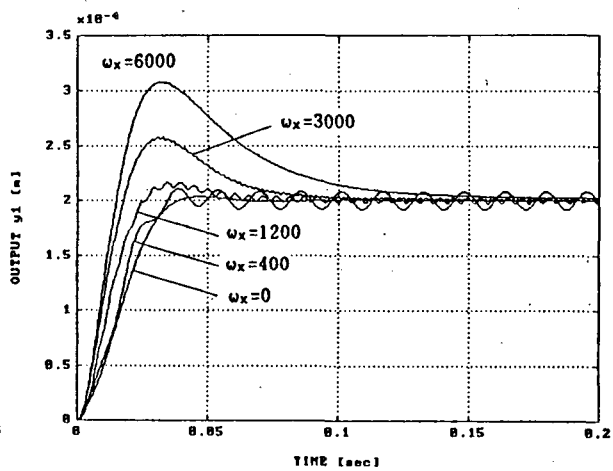


(d) Centralized PID Servocompensator:  
Axis Trajectory

Fig.5 Simulation Results for Sinusoidal Reference Tracking  
(  $y_{1ref}=0.0002\sin(400t)[m]$ ,  $y_{2ref}=-0.0002\sin(400t)[m]$ ,  $F_{dy}=-1000[N]$ ,  
 $z_{1ref}=0.0002\cos(400t)[m]$ ,  $z_{2ref}=-0.0002\cos(400t)[m]$  )



(a) General Servocompensator



(b) Centralized PID Servocompensator

Fig.6 Robustness Comparison of Two Types of Control Schemes

In Fig.6, the robustness of two types of control schemes is compared. The reference and disturbance signals are same as in Fig.4. The regulating function is tested for the whole range of  $\omega_x$  with the control gains maintained as a same set as those obtained at  $\omega_x = 400$  [r/s]. Since the characteristics of the open-loop system changes as  $\omega_x$  varies [Fig.3], the degree of robustness can be verified. It is very clear that the centralized PID controller shows an asymptotical stability up to the range of 6000 r/s and more. However, the bandwidth of the general servocompensator gets decreased as  $\omega_x$  increases. The allowable plant model variations are limited in case of general servocompensator.

## 5. CONCLUSION

A robust control theory is applied to obtain two types of centralized control schemes for a rigid rotor system supported by magnetic bearings. The negative stiffness and inductive force effect are included in the plant model and no local feedback action is assumed. The control scheme which utilizes a general servocompensator reveals perfect tracking and regulation for the sinusoidal reference and disturbance signals, whereas the robustness is limited. The centralized PID control scheme maintains the asymptotical stability up to the spinning speed of 6000 r/s, hence reveals good robustness.

## REFERENCES

1. Higuchi, T., T. Mizuno and T. Tsukamoto, 1990. "Digital Control System for Magnetic Bearings with Automatic Balancing." 2nd Int. Symposium on Magnetic Bearing, Tokyo, Japan, pp27-32.
2. Larocca, P., D. Fermental and E. Cusson, 1990. "Performance Comparison between Centralized and Decentralized Control of the Jeffcott Rotor." 2nd Int. Symposium on Magnetic Bearing, Tokyo, Japan, pp295-300.
3. Youcef-Toumi, K., S. Reddy and I. Vithianathan, 1990. "A Digital Time Delay Controller for Active Magnetic Bearings." 2nd Int. Symposium on Magnetic Bearing, Tokyo, Japan, pp15-21.
4. Davison, E. J., 1976. "The Robust Control of a Servomechanism Problem for Linear Time-invariant Multivariable Systems." IEEE Trans. on Automatic Control, Vol AC-21, No.1, pp25-34.
5. Davison, E. J. and I. J. Ferguson, 1981. "The Design of Controllers for the Multivariable Robust Servomechanism Problem Using Parameter Optimization Methods." IEEE Trans. on Automatic Control, Vol. AC-26, No.1, pp93-110.
6. Davison, E. J. and W. Gesing, 1978. "An Algorithm for Obtaining the Minimal Realization of a Linear Time-invariant System and Determining if a System is Stabilizable-Detectable." IEEE Trans. on Automatic Control, Vol. AC-23, No.6, pp1048-1054.
7. Fermental, D., E. Cusson and P. Larocca, 1990. "A Decomposition of the Jeffcott Rotor." 2nd Int. Symposium on Magnetic Bearing, Tokyo, Japan, pp289-294.